Localized suppression of longitudinal-optical-phonon–exciton coupling in bent ZnO nanowires

2010 Nanotechnology 21 445706

(http://iopscience.iop.org/0957-4484/21/44/445706)

Nanotechnology **21** (2010) 445706 (6pp) doi:10.1088/0957-4484/21/44/445706

Localized suppression of longitudinal-optical-phonon–exciton coupling in bent ZnO nanowires

Bin Yan[1], Rui Chen[1], Weiwei Zhou[1], Jixuan Zhang[2], Handong Sun[1], Hao Gong[2] and Ting Yu[1,3]

[1] Division of Physics and Applied Physics, School of Physical and Mathematical Sciences, Nanyang Technological University, 637371, Singapore
[2] Department of Materials Science and Engineering, Faculty of Engineering, National University of Singapore, 117574, Singapore

E-mail: yuting@ntu.edu.sg

Received 19 July 2010, in final form 21 September 2010
Published 8 October 2010
Online at stacks.iop.org/Nano/21/445706

Abstract
Using confocal micro-Raman and photoluminescence spectroscopy, we studied bending effects on optical properties of individual ZnO nanowires. Raman spectroscopy shows that local tensile strain can be introduced by bending the nanowire. The strain is expected to reduce the band gap on the bent part and modify the local phonon–exciton interaction. The corresponding micro-photoluminescence spectra indicate local suppression of the longitudinal-optical (LO) phonon–exciton interaction, which is determined by the intensity ratio of the second-order LO-phonon replica of the free exciton (FX–2LO) to the first-order process (FX–1LO). Our results may provide insight into the modulation of local electrical and optical properties by deforming the nanostructures.

(Some figures in this article are in colour only in the electronic version)

1. Introduction

Combined with the chemical stability, the high flexibility of metal-oxide nanowires enables them to be one of the most promising components for elastic optoelectronics [1–4]. One of the important issues under intensive investigation is the bending effect, which is a typical deformation that occurs in the flexible devices [5]. In particular, Wang proposed that a lateral electrical potential can be achieved by bending the ZnO nanowire due to its piezoelectric property [6]. This kind of piezoelectric effect may influence the electrical transport characteristics of the nanowire-based field-effect transistor (FET) [1]. In addition, tensile or compressive strains are expected to benefit from the bowing of nanowires, which could modulate the energy band structure [7, 8] and the carrier effective mass [9]. However, relatively less effort has been devoted to optical properties of the curved ZnO nanowires [7], especially effects on the phonon–exciton interaction. As it is a polar semiconductor, ZnO experiences a strong Fröhlich interaction (FI) that gives rise to longitudinal-optical (LO) phonon–exciton interaction. Herein, the coupling between exciton and phonon along the bent nanowire was investigated by confocal micro-photoluminescence spectroscopy.

2. Experiment

The ZnO nanowire samples used in this study were synthesized on silicon substrates by a Au-catalyst-assisted chemical vapor deposition method in a horizontal tube furnace [10]. The large aspect ratio and elastic flexibility allowed manipulation of the location and shape of individual nanowires under the optical microscope using a commercial micromanipulator tipped with sharp tungsten probes. The morphological and crystal structures were characterized by scanning electron microscopy (SEM) (JEOL JSM-6700F) and transmission electron microscopy (TEM) (200 kV JEOL 2010F). The temperature-dependent PL measurement of the as-fabricated samples was performed between 10 and 300 K within a closed-cycle helium cryostat and a He–Cd laser (325 nm) was used

[3] Author to whom any correspondence should be addressed.

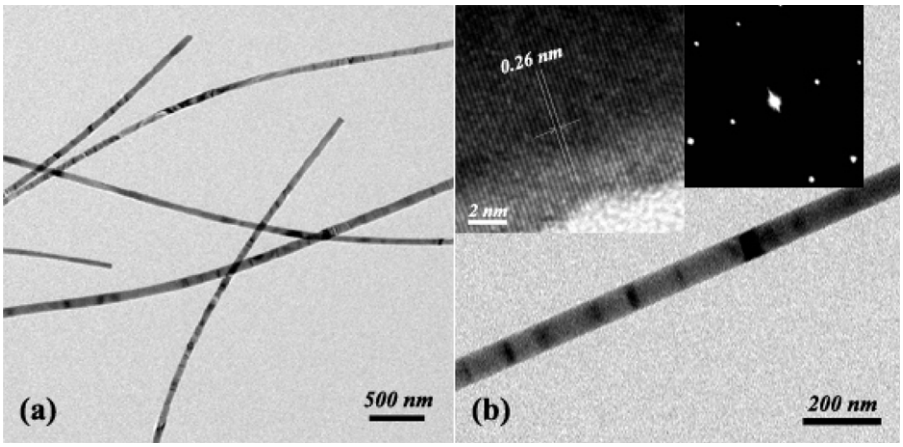

Figure 1. (a) TEM images of the ZnO nanowires. (b) High-magnification TEM and the corresponding selected area electron diffraction (SAED) pattern.

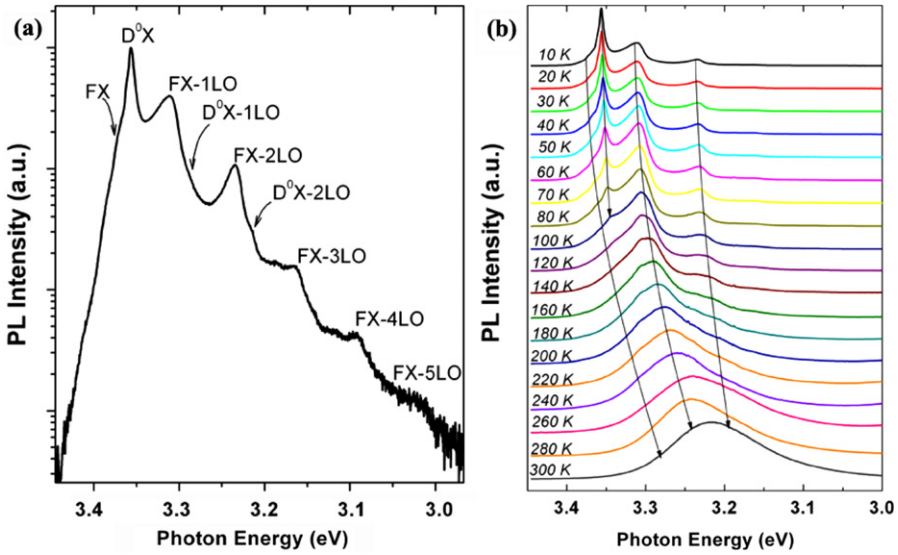

Figure 2. (a) UV emission of the as-grown sample at 10 K. (b) Temperature-dependent photoluminescent properties of the sample. The evolutions of the FX, D^0X, FX–1LO and FX–2LO peaks are indicated by solid lines.

for excitation. The micro-photoluminescence and Raman spectra of individual nanowires were measured using the same laser line and a confocal Raman microscope (inVia Renishaw Raman) at room temperature. The spot size is about 1 μm with low excitation power density to avoid laser-induced heating effects in the sample.

3. Results and discussion

Figure 1(a) shows the TEM images of the samples. The diameter of the ZnO nanowires is about 50 nm, with a smooth surface. The *d*-spacing of 0.26 nm from high resolution TEM (figure 1(b)) corresponds to the lattice spacing of (0001) planes of wurtzite ZnO. At low temperature (10 K), the PL spectrum of the as-grown sample exhibits several peaks (as shown in figure 2(a)), which correspond to the free-exciton (FX) emission, the neutral-donor-bound exciton (D^0X) emission, and their LO-phonon replicas separated by a constant energy interval of 72±2 meV. FX–*n*LO transitions are more dominant than D^0X–*n*LO transitions, which indicates that the coupling of the FX to the LO phonon is stronger than that between D^0X and LO phonons. Besides, up to fifth-order phonon replicas of free-exciton emission could be distinguished, showing the high crystalline quality and strong coupling of phonon and exciton in our ZnO nanowires. Figure 2(b) depicts the temperature-dependent PL spectra of the as-grown sample. As temperature increases, the intensities of D^0X-related emissions decrease much faster than those of FX and FX–*n*LO due to the thermal activation of the donor-bound exciton, and finally the FX and its first two replica transitions are dominant at room temperature. This strong coupling between the FX and LO phonon provides a possibility to investigate the bending effect on exciton–phonon interactions by deconvolution analysis of the spectra [11–13], which will be discussed later.

The micro-Raman technique is used to probe the local strain effect on an individual nanowire. A typical bent ZnO

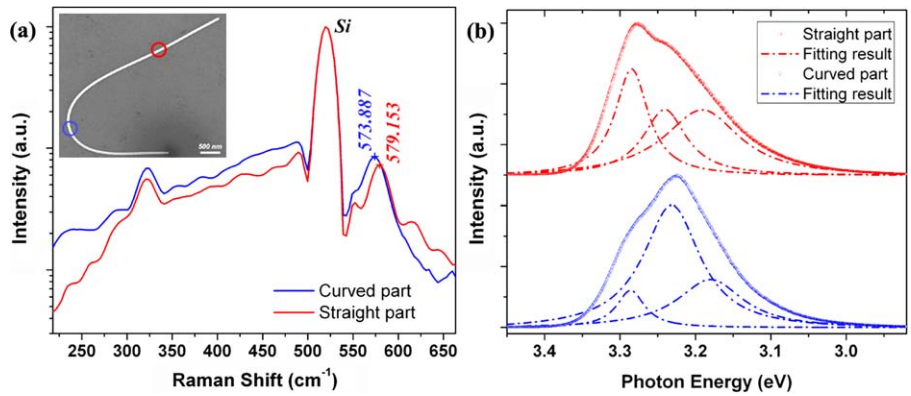

Figure 3. (a) Normalized Raman spectra acquired at different positions of the bent ZnO nanowire. Inset: SEM image of a strongly curved ZnO nanowire. (b) Deconvolution analysis for the corresponding PL spectra from the straight and curved parts.

nanowire of 56 nm in diameter, 8 μm in length is shown in the inset of figure 3(a). The Raman spectra acquired at different positions are summarized using semi-logarithmic coordinates (figure 3(a)). All spectra display two clear phonon modes which can be associated with the Si substrate Raman peak at 520 cm^{-1} and the LO phonon of ZnO. At the straight part of the ZnO nanowire, the peak position of the LO phonon mode is found at 579 cm^{-1}, close to the value expected for wurtzite ZnO [14]. At that position, the full width at half maximum (FWHM) is about 21.82 cm^{-1}. For the curved part of the nanowire, it displayed a significant shift of the phonon energy toward lower frequencies (574 cm^{-1}) with a FWHM of 22.58 cm^{-1}. As known, the LO phonon in ZnO is very sensitive to the strain and formation of defects [15]. Compressive and tensile stresses of the sample will shift the phonon peak to a higher and a lower wavenumber, respectively, while the presence of structural defects is expected to broaden the Raman peaks. In this case, we can claim that local tensile strain can be introduced by bending the nanowire without obvious crack defects and such a bending deformation is elastic.

In an ideal case, the nanowire is expected to experience simultaneous compressive strain on the inner side of the curvature and tensile strain on the outer side, while the central area is free of strain. So that the Raman peak at the bending part should be symmetrically broadened with no shift of peak position [16]. However, it is found that the strain distribution is very dependent on the materials and different loading conditions. For example, for Ge, the compressive strength is expected to be an order of magnitude larger than the tensile strength [17]. Meanwhile, as we manipulated the nanowire on the silicon substrate, surface forces, such as adhesion and friction forces [18] between nanowires and substrate, could also influence the strain distribution. In our experiment, the LO Raman mode shifts toward lower wavenumbers, revealing the domination of tensile stress at the curved part of ZnO under the bending effect. So we proposed that the outer wall of the nanowire would suffer more deformation than the inner part, resulting in tensile strain dominance. As the laser spot is large compared to the diameter of the nanowire, the detailed mechanism of the bending-induced tensile strain requires further study.

The tensile strain that we have observed experimentally from Raman scattering should result in some local effects on the electronic states and exciton–phonon interaction. Band gap shrinkage induced by tensile strain in ZnO has been realized recently [7]. Of special interest in this study is the exciton–phonon coupling at the curved part of the nanowire. The corresponding micro-photoluminescence spectra were collected as shown in figure 3(b). In order to quantify the relative contributions of the FX and its phonon replica processes to the room-temperature PL, the spectra from both the straight and bent parts of the nanowire were well fitted by three Lorentzian peaks [11–13], which determined the contribution of FX, FX–1LO and FX–2LO (as discussed before). No obvious peak interval variability was observed for different positions. Generally, the emission intensity of the nth phonon replica I_n and the zero-phonon line I_0 are related by

$$I_n = \frac{S^n}{n!} I_0.$$

S is the so called Huang–Rhys factor, which provides a quantitative description of the exciton–phonon coupling property. However, it was found that the ratio $I_{\mathrm{FX-1LO}}/I_{\mathrm{FX}}$ can lead to erroneous conclusions about the Huang–Rhys factor, as the zero-phonon band may consist of several decay resources [19, 20]. Thus, we make a rough estimation of exciton–phonon coupling by the intensity ratio of FX–2LO to FX–1LO emission.

As shown in figure 3(b), the FX emission is suppressed compared to its first LO-phonon replica for the strongly bent region. We tentatively ascribed it to the bending-induced defects or traps. Excitons can decay nonradiatively via defect states. In this case, the reduction of FX–1LO emission may be smaller than that of FX emission considering the fast relaxation time of the LO-phonon emission [21], and defects can even increase/influence the relative intensity of 1LO-phonon scattering [22, 23]. The significant suppression of the FX emission compared to the FX–1LO emission can be associated with the dissociation of the exciton which might enhance the conductivity of the nanowire [24], but still requires further detailed studies. Combined with the redshift of FX emission, the enhanced contribution of FX–1LO leads to a

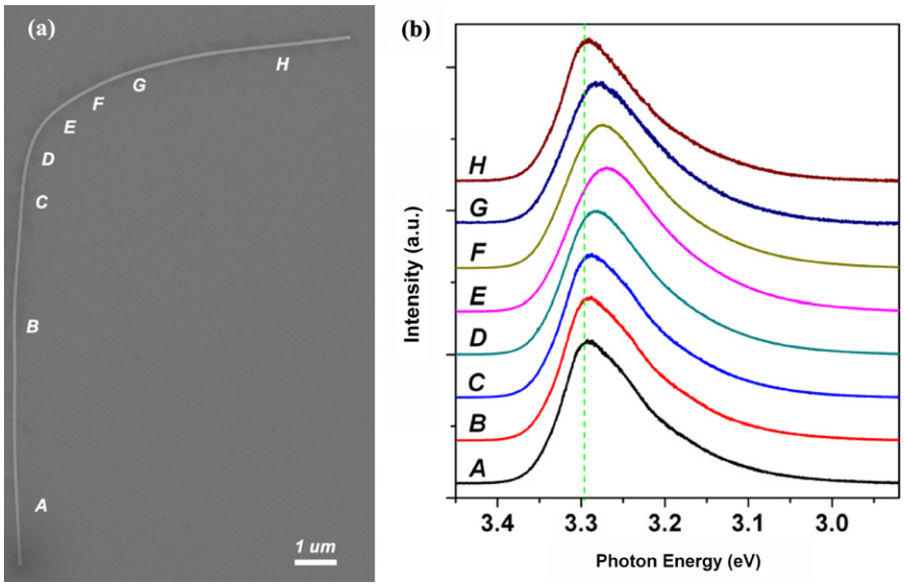

Figure 4. (a) SEM image of an individual bent ZnO nanowire dispersed on a SiO_2/Si substrate. (b) PL spectra collected from different positions of the nanowire.

remarkable change of the emission profile. And the ratio of FX–2LO to FX–1LO in the curved part was decreased to one fourth of that observed in the straight part, which attests to the weakening coupling strength of the exciton to the LO phonon as the nanowire is bent. So the comparison between figures 3(a) and (b) provides a new insight in such a relationship: tensile strain, induced by bending the nanowire, is expected to suppress the local exciton–LO-phonon coupling.

To confirm this, spatially resolved PL spectra along the axis of a long nanowire were performed using a confocal micro-spectrometer at room temperature. The diameter of the nanowire is 60 nm with 20 μm length (shown in figure 4(a)), illustrating the extreme flexibility of the nanowires. As shown in figure 4(b), the spectra collected from the positions *A* and *H* exhibit similar lineshapes. So we can deduce that the profile of UV emission is not affected much by the anisotropic orientation of the nanowires, even if the strength can be polarization dependent stemming from the dielectric mismatch between the nanowires and their local surrounding environment [25–27]. When going from the spectra collected at the straight part to those at the curved part, as a general trend, the line width decreases as the peak energy position shifts towards lower energies. The local PL spectra present at least two important points. First, the near-band-edge peak position shows significant bending-induced redshift. Second, the spectrum profile changes accompanied with macroscopic bending of the nanowire. From the fitting results, figure 5 plots the peak energy of the FX corresponding to the different positions along the bent nanowire. In contrast to the normal pressure-induced blue-shift [28–30], an obvious redshift can be observed for the near-band-edge FX emission. In this case, we proposed that a uniaxial tensile strain can be dominant when a bending deformation is applied on the ZnO nanowire, which is in good agreement with our Raman measurement and theoretical predictions from [7]. As shown in figure 5, the

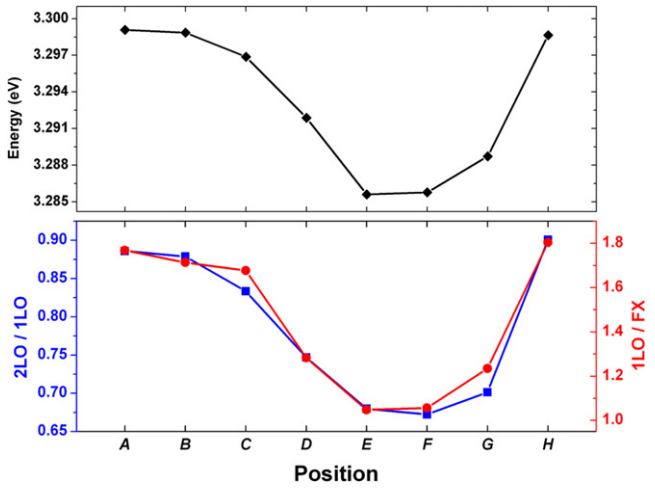

Figure 5. Photon energy of the FX, I_{2LO}/I_{1LO} and I_{1LO}/I_{FX} as a function of position along the nanowire.

I_{2LO}/I_{1LO} decreases with increasing the curvature. More than 20 nanowires were investigated, and all of them show the same behavior. In addition, for most of the samples, the same trend can be observed for I_{1LO}/I_{FX}. All these results indicate the reduction of exciton–LO-phonon interaction on the bending ZnO nanowires. In the future, micro-PL measurements at low temperature can be expected. This kind of difference in the strength of exciton–phonon coupling could have significant effects on the optical and transport properties of electrons in semiconductors [31, 32]. We also tried to investigate the effect of bend radius, and nanowire thickness. However, due to the instrumental resolution, we could not get a quantitative conclusion.

For advanced study, we have also collected the second-order Raman spectra of the LO phonon from different positions on a nanowire. Careful analysis of the resonant Raman

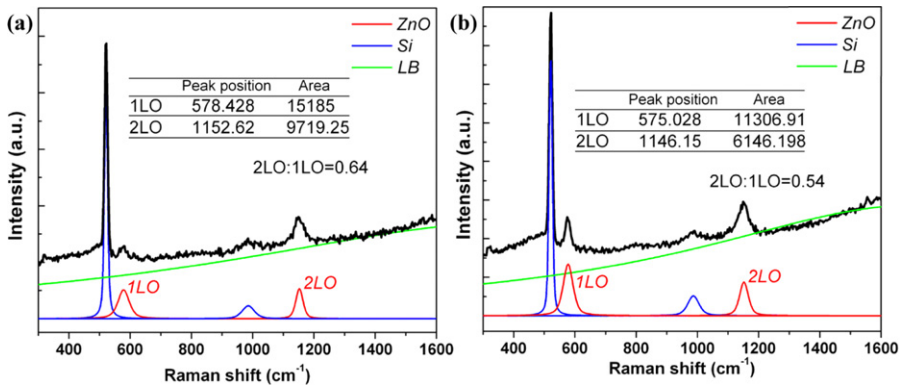

Figure 6. UV resonant Raman modes from straight (a) and bending (b) parts of an individual nanowire.

spectrum was performed by the peak fitting, as shown in figure 6. The inset table summarizes the relevant data for the ZnO LO-phonon Raman bands. As we can see, the position of the LO phonon from the bending part is shifted due to the tensile strain effect. Even if there is an obvious photo-induced luminescence baseline (LB), the ratio of LO overtone is significantly reduced from 0.64 to 0.54, which is consistent with the trend we observed in micro-PL studies. More confident evidence can be expected using resonant Raman mapping and low-temperature micro-photoluminescence measurement.

It should be pointed out that for the optical phonon both the deformation potential (microscopic distortions) and the Fröhlich interaction can contribute to the matrix element of exciton–phonon interaction [32]. Through the uniaxial tensile strain (which will lead to the increase of the lattice constant along the c-axis), the microscopic relative displacement (u/c_0, where c_0 is the distance between the two atoms inside the primitive unit cell, and u is the relative displacement between atoms along the c-axis associated with the A_1(LO) phonon) of the charged atoms within the primitive cell decreases with increasing the bending deformation. So the phonon–exciton interaction can be reduced. Another reason for the decreased coupling is the changed confining potentials for the electron and hole wavefunction. For an exciton the polar coupling strength is proportional to the squared absolute value of the Fourier transformed difference of the probability densities of electron and hole [33]. With decreasing diameter the influence of surface-related effects becomes increasingly important. Wang *et al* [6] reported that an electric potential can be produced by the piezoelectric effect and the trapping of electrons at the curved interfaces of the nanowire. This effect might result in an influence of the confining potential on the exciton wavefunction, especially for the surface region. In this case, it makes the exciton less polar, reducing the coupling strength with the polar lattice via the Fröhlich interaction. On the other hand, taking into account the bending-induced surface defects, the trapping of excitons at surface located defects results in a reduction of the excited-state lifetime, which can cause a decrease of the exciton–phonon coupling [34]. Though the presented model might be considered to be very crude, it can be regarded as a first step for further study of the local interplay between the mechanical deformation and the exciton–phonon coupling in one-dimensional nanostructures.

4. Conclusion

In summary, the micro-Raman and photoluminescent properties of individual bent ZnO nanowires were studied. The presence of tensile strain was analyzed by the relative shift of the phonon modes. Using spatially resolved PL experiments, it is found that the ratio of FX–2LO to FX–1LO emission can be suppressed in nanowires due to the bending effect. The possibility to engineer the local phonon–exciton coupling by curving the nanowire provides a unique approach to optimizing the electrical and optical properties of a semiconductor nanostructure.

References

[1] Kwon S S, Hong W K, Jo G, Maeng J, Kim T W, Song S and Lee T 2008 *Adv. Mater.* **20** 4557–62
[2] Ju S Y, Facchetti A, Xuan Y, Liu J, Ishikawa F, Ye P D, Zhou C W, Marks T J and Janes D B 2007 *Nat. Nanotechnol.* **2** 378–84
[3] Nadarajah A, Word R C, Meiss J and Konenkamp R 2008 *Nano Lett.* **8** 534–7
[4] Yan B, Liao L, You Y M, Xu X J, Zheng Z, Shen Z X, Ma J, Tong L M and Yu T 2009 *Adv. Mater.* **21** 2436–40
[5] Baca A J, Ahn J H, Sun Y G, Meitl M A, Menard E, Kim H S, Choi W M, Kim D H, Huang Y and Rogers J A 2008 *Angew. Chem. Int. Edn* **47** 5524–42
[6] Wang Z L and Song J H 2006 *Science* **312** 242–6
[7] Han X B *et al* 2009 *Adv. Mater.* **21** 4937–41
[8] He R R and Yang P D 2006 *Nat. Nanotechnol.* **1** 42–6
[9] Shiri D, Kong Y, Buin A and Anantram M P 2008 *Appl. Phys. Lett.* **93** 073114
[10] Fan H J, Werner P and Zacharias M 2006 *Small* **2** 700–17
[11] Ahn C H, Mohanta S K, Lee N E and Cho H K 2009 *Appl. Phys. Lett.* **94** 261904
[12] Hong W K, Jo G, Choe M, Lee T, Sohn J I and Welland M E 2009 *Appl. Phys. Lett.* **94** 043103
[13] Voss T, Bekeny C, Wischmeier L, Gafsi H, Borner S, Schade W, Mofor A C, Bakin A and Waag A 2006 *Appl. Phys. Lett.* **89** 182107
[14] Scott J F 1970 *Phys. Rev.* B **2** 1209–11
[15] Ng H T, Chen B, Li J, Han J E, Meyyappan M, Wu J, Li S X and Haller E E 2003 *Appl. Phys. Lett.* **82** 2023–5
[16] Chen J, Conache G, Pistol M-E, Gray S M, Borgström M T, Xu H, Xu H Q, Samuelson L and Håkanson U 2010 *Nano Lett.* **10** 1280–6

[17] Smith D A, Holmberg V C and Korgel B A 2010 *ACS Nano* **4** 2356–62
[18] Desai A V and Haque M A 2007 *Appl. Phys. Lett.* **90** 033102
[19] Brener I, Olszakier M, Cohen E, Ehrenfreund E, Ron A and Pfeiffer L 1992 *Phys. Rev.* B **46** 7927–30
[20] Kundrotas J, Cerskus A, Asmontas S, Valusis G, Halsall M P, Johannessen E and Harrison P 2007 *Semicond. Sci. Technol.* **22** 1070–6
[21] Ueta M 1986 *Excitonic Processes in Solids* (Berlin: Springer)
[22] Cho Y H, Kim J Y, Kwack H S, Kwon B J, Dang L S, Ko H J and Yao T 2006 *Appl. Phys. Lett.* **89** 201903
[23] Lucca D A, Hamby D W, Klopfstein M J and Cantwell G 2002 *Phys. Status Solidi* b **229** 845–8
[24] Han X B, Jing G Y, Zhang X Z, Ma R M, Song X F, Xu J, Liao Z, Wang N and Yu D 2009 *Nano Res.* **2** 553–7
[25] Wang J F, Gudiksen M S, Duan X F, Cui Y and Lieber C M 2001 *Science* **293** 1455–7
[26] Ruda H E and Shik A 2005 *Phys. Rev.* B **72** 115308
[27] Yan B, Du C L, Liao L, You Y M, Cheng H, Shen Z X and Yu T 2010 *Appl. Phys. Lett.* **96** 073105
[28] Shan W, Walukiewicz W, Ager J W, Yu K M, Zhang Y, Mao S S, Kling R, Kirchner C and Waag A 2005 *Appl. Phys. Lett.* **86** 153117
[29] Su F H, Wang W J, Ding K, Li G H, Liu Y F, Joly A G and Chen W 2006 *J. Phys. Chem. Solids* **67** 2376–81
[30] Chen S J, Liu Y C, Shao C L, Xu C S, Liu Y X, Liu C Y, Zhang B P, Wang L, Liu B B and Zou G T 2006 *Appl. Phys. Lett.* **88** 133127
[31] Lee S and Kim D Y 2008 *J. Appl. Phys.* **104** 093515
[32] Yu P Y and Cardona M 2005 *Fundamentals of Semiconductors, Physics and Materials Properties* (Berlin: Springer)
[33] Heitz R, Mukhametzhanov I, Stier O, Madhukar A and Bimberg D 1999 *Phys. Rev. Lett.* **83** 4654–7
[34] Shiang J J, Risbud S H and Alivisatos A P 1993 *J. Chem. Phys.* **98** 8432–42